LA-UR-15-26810
Approved for public release; distribution is unlimited.

Title: On-the-Fly Nuclear Data Processing Methods for Monte Carlo Simulations of Fast Spectrum Systems

Author(s): Walsh, Jon

Intended for: Document Summer R&D work on Monte Carlo

Issued: 2015-08-31

On-the-Fly Nuclear Data Processing Methods for Monte Carlo Simulations of Fast Spectrum Systems

Jon Walsh

Computational Reactor Physics Group (CRPG)
Department of Nuclear Science & Engineering
Massachusetts Institute of Technology

XCP-3 Group Meeting

August 19, 2015

Section 1

Unresolved Resonance Region

Guiding Objectives

High-fidelity, precise Monte Carlo simulations of realistic intermediate and fast spectrum systems

1. Improved physics
   - Representation of nuclear data
   - Processing methods

Guiding Objectives

High-fidelity, precise Monte Carlo simulations of realistic intermediate and fast spectrum systems

1. Improved physics
   - Representation of nuclear data
   - Processing methods
2. Computational efficiency
   - Memory requirements
   - Calculation speed

Unresolved Resonance Region

- Intermediate-energy resonances can be experimentally unresolvable
- Nuclear data evaluators give us average information about cross section behavior in the URR
- Associated theoretical statistical distributions are known
- In nature, fine structure still exists

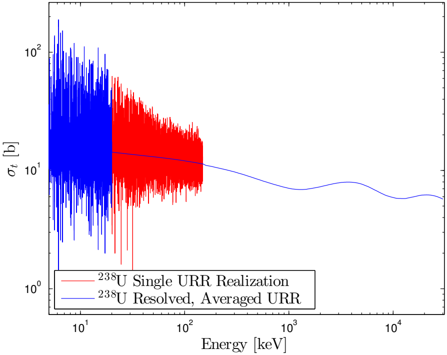

Figure : ^{238}U total cross section at 293.6 K

Averaged Pointwise Cross Sections

- A known, pointwise cross section is just a collapsed distribution,

$$\sigma_x(E) = \langle \sigma_x(E) \rangle = \int_{-\infty}^{\infty} d\sigma'_x \delta(\sigma'_x - \sigma_x(E))\sigma'_x \tag{1}$$

- More generally, we can't collapse (resolve) the distribution to a point, so we have a Lebesgue integral in σ'_x-space,

$$\langle \sigma_x(E) \rangle = \int_{-\infty}^{\infty} d\sigma'_x P(\sigma'_x | E)\sigma'_x \tag{2}$$

- This is what we have to deal with in the URR

URR Self-Shielding Effects

- Averaging process is equivalent to generation of infinite-dilute cross sections
- No resonance structure
  $\rightarrow$ No flux perturbation
  $\rightarrow$ No energy self-shielding

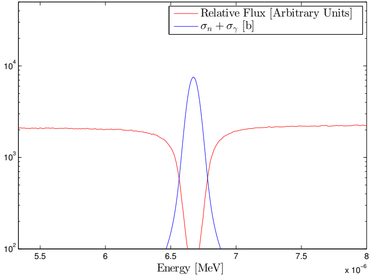

Figure : Energy self-shielding schematic

URR Self-Shielding Effects

- Averaging process is equivalent to generation of infinite-dilute cross sections
- No resonance structure
  $\rightarrow$ No flux perturbation
  $\rightarrow$ No energy self-shielding
- Mis-predicted reaction rates
- Artificially high resonance absorption
- Under-predicted k_{eff} eigenvalues
- Unconservative critical assembly calculations

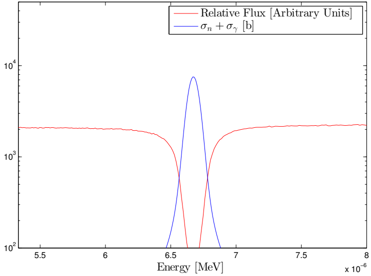

Figure : Energy self-shielding schematic

URR Self-Shielding Effects

- Averaging process is equivalent to generation of infinite-dilute cross sections
- No resonance structure
  $\rightarrow$ No flux perturbation
  $\rightarrow$ No energy self-shielding
- Mis-predicted reaction rates
- Artificially high resonance absorption
- Under-predicted k_{eff} eigenvalues
- Unconservative critical assembly calculations

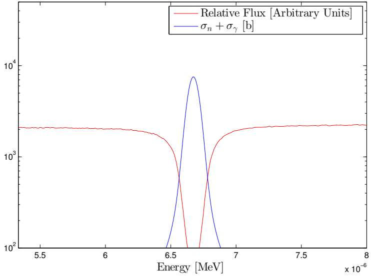

Figure : Energy self-shielding schematic

- Resonance overlap can exacerbate the effect

URR Self-Shielding Effects

- Averaging process is equivalent to generation of infinite-dilute cross sections
- No resonance structure
  $\rightarrow$ No flux perturbation
  $\rightarrow$ No energy self-shielding
- Mis-predicted reaction rates
- Artificially high resonance absorption
- Under-predicted k_{eff} eigenvalues
- Unconservative critical assembly calculations

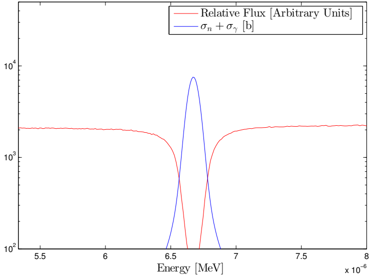

Figure : Energy self-shielding schematic

- Resonance overlap can exacerbate the effect
- Fine structure in the URR needs to be represented

Probability Table Method

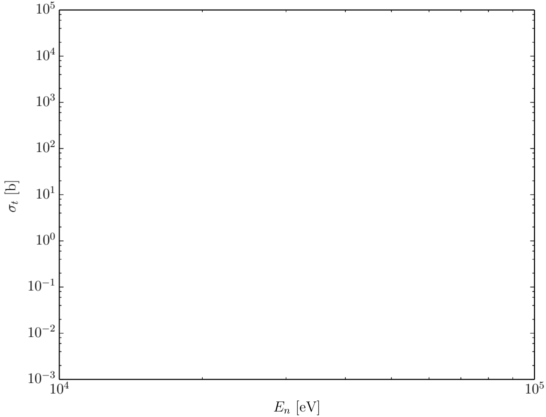

- Need σ_t magnitudes as a function of E_n and T

Probability Table Method

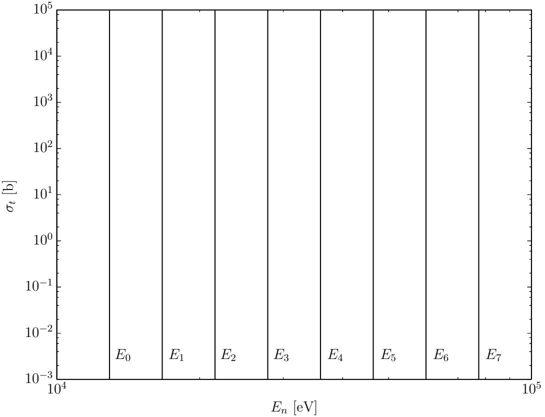

- At each discrete T, set an E_n mesh

Probability Table Method

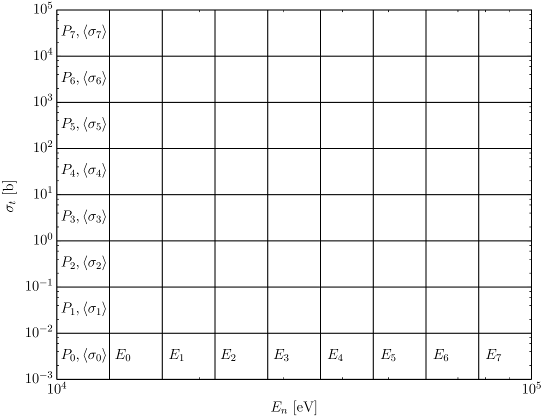

- At each discrete E_n, set a σ_t mesh

Probability Table Method

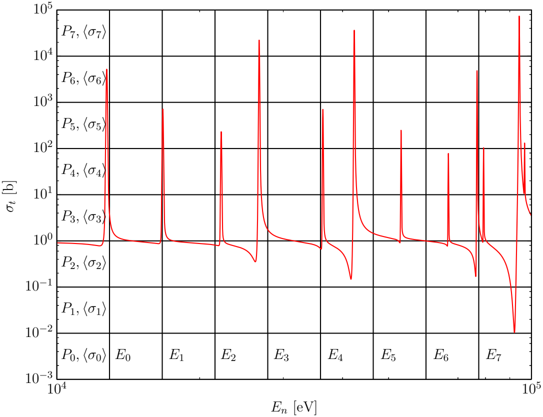

- Randomly generate an independent realization of resonance structure

Probability Table Method

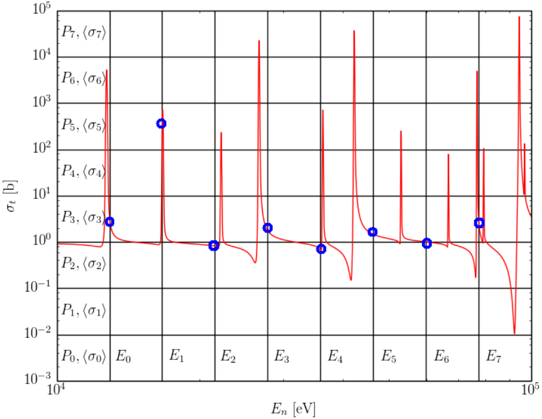

- Record band index and magnitude at each E_n
- Average over all samples to compute band probability and σ_t

Probability Table Method

- Stochastically generated tables of cross section values with associated probabilities of being realized at discrete energies **AND** temperatures
- Cross section values, $\{\hat{\sigma}_x^1(E_i), \hat{\sigma}_x^2(E_i), ..., \hat{\sigma}_x^J(E_i)\}$, are sampled according to their associated probabilities, $\{\hat{P}_t^1(E_i), \hat{P}_t^2(E_i), ..., \hat{P}_t^J(E_i)\}$, as necessary, throughout the transport simulation

Probability Table Method

- Stochastically generated tables of cross section values with associated probabilities of being realized at discrete energies **AND** temperatures
- Cross section values, $\{\hat{\sigma}_x^1(E_i), \hat{\sigma}_x^2(E_i), ..., \hat{\sigma}_x^J(E_i)\}$, are sampled according to their associated probabilities, $\{\hat{P}_t^1(E_i), \hat{P}_t^2(E_i), ..., \hat{P}_t^J(E_i)\}$, as necessary, throughout the transport simulation
- Well-established method for treating URR cross section resonance structure
- Implemented in several nuclear data pre-processing codes (NJOY, PREPRO, PROTAB/RACER, CALENDF, AMPX, and others)

Probability Table Method

- Stochastically generated tables of cross section values with associated probabilities of being realized at discrete energies **AND** temperatures
- Cross section values, $\{\hat{\sigma}_x^1(E_i), \hat{\sigma}_x^2(E_i), ..., \hat{\sigma}_x^J(E_i)\}$, are sampled according to their associated probabilities, $\{\hat{P}_t^1(E_i), \hat{P}_t^2(E_i), ..., \hat{P}_t^J(E_i)\}$, as necessary, throughout the transport simulation
- Well-established method for treating URR cross section resonance structure
- Implemented in several nuclear data pre-processing codes (NJOY, PREPRO, PROTAB/RACER, CALENDF, AMPX, and others)
- Drawbacks include opaqueness of the generation process, the need for sensitivity/mesh refinement studies, and increased memory requirements

Section 2

On-the-Fly Cross Sections

Calculating URR Cross Sections On-the-Fly

- Average resonance parameter values given for energy ranges

Calculating URR Cross Sections On-the-Fly

- Average resonance parameter values given for energy ranges
- Sample the theoretical distributions of those parameters

Calculating URR Cross Sections On-the-Fly

- Average resonance parameter values given for energy ranges
- Sample the theoretical distributions of those parameters
- Generate energy-localized resonance realizations (i.e. level spacings and partial widths) at each event

Calculating URR Cross Sections On-the-Fly

- Average resonance parameter values given for energy ranges
- Sample the theoretical distributions of those parameters
- Generate energy-localized resonance realizations (i.e. level spacings and partial widths) at each event
- Compute temperature-dependent SLBW resonance cross sections via $\psi - \chi$ Doppler integrals

Calculating URR Cross Sections On-the-Fly

- Average resonance parameter values given for energy ranges
- Sample the theoretical distributions of those parameters
- Generate energy-localized resonance realizations (i.e. level spacings and partial widths) at each event
- Compute temperature-dependent SLBW resonance cross sections via $\psi - \chi$ Doppler integrals
- Continuous phase-space (E_n, T, σ) analog to probability tables

Calculating URR Cross Sections On-the-Fly

- Average resonance parameter values given for energy ranges
- Sample the theoretical distributions of those parameters
- Generate energy-localized resonance realizations (i.e. level spacings and partial widths) at each event
- Compute temperature-dependent SLBW resonance cross sections via $\psi - \chi$ Doppler integrals
- Continuous phase-space (E_n, T, σ) analog to probability tables
- **Proceeds directly from temperature-independent resonance parameters**

Level Spacings

"Wigner's surmise" for distribution of level spacings:

$$P_W\left(\frac{D_{l,J_j}}{\langle D_{l,J_j}(E_n)\rangle}\right) = \frac{\pi D_{l,J_j}}{2\langle D_{l,J_j}(E_n)\rangle}\exp\left(-\frac{\pi D_{l,J_j}^2}{4\langle D_{l,J_j}(E_n)\rangle^2}\right) \quad (3)$$

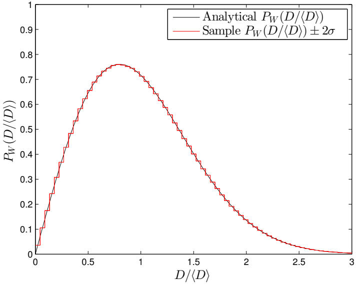

Figure : Sampled and analytical level spacing distributions

Partial Widths

Partial reaction widths, Γ_r, are obtained by sampling a χ^2 distribution:

$$P_{\chi^2(\mu_r)}(y) = \frac{\exp\left(-\frac{y}{2}\right) y^{\frac{\mu_r}{2}-1}}{2^{\mu_r/2} G\left(\frac{\mu_r}{2}\right)}; \qquad y \equiv \mu_r \frac{\Gamma_r^{l,J}}{\langle \Gamma_r^{l,J}(E_n) \rangle} \tag{4}$$

Construction of a discrete distribution with N equiprobable bins:

$$\int_{y_{i-1}}^{y_i} P_{\chi^2(\mu_r)}(y')dy' = \frac{1}{N}; \quad i = 1, 2, ..., N; \quad y_0 = 0; \quad y_N \to \infty \tag{5}$$

$$\langle y' \rangle_i = N \int_{y_{i-1}}^{y_i} y' P_{\chi^2(\mu_r)}(y')dy' \tag{6}$$

Single-Level Breit-Wigner Formulae

- Elastic scattering:

$$\sigma_n(E_n) = \sum_{l=0}^{NLS-1} \sum_{j=1}^{NJS_l} \sum_{\lambda=1}^{N_{\mathrm{res}}} \sigma_\lambda \left(\left[\cos\left(2\phi_l(\rho)\right) - \left(1 - \frac{\Gamma_{n,\lambda}}{\Gamma_\lambda}\right) \right] \psi(\theta, x) + \chi(\theta, x) \sin\left(2\phi_l(\rho)\right) \right) + \frac{4\pi}{k(E_n)^2} \sum_{l=0}^{NLS-1} (2l+1) \sin^2\left(\phi_l(\rho)\right) \tag{7}$$

- Reaction:

$$\sigma_r(E_n) = \sum_{l=0}^{NLS-1} \sum_{j=1}^{NJS_l} \sum_{\lambda=1}^{N_{\mathrm{res}}} \sigma_\lambda \frac{\Gamma_{r,\lambda}}{\Gamma_\lambda} \psi(\theta, x) \tag{8}$$

- $\psi - \chi$ Doppler integrals:

$$\psi(\theta, x) = \frac{\theta\sqrt{\pi}}{2} \mathrm{Re}\left[W\left(\frac{\theta x}{2}, \frac{\theta}{2}\right)\right]; \qquad \chi(\theta, x) = \frac{\theta\sqrt{\pi}}{2} \mathrm{Im}\left[W\left(\frac{\theta x}{2}, \frac{\theta}{2}\right)\right] \tag{9}$$

- Faddeeva function:

$$W(\alpha, \beta) = \exp\left(-z^2\right) \mathrm{erfc}\left(-iz\right) = \frac{i}{\pi} \int_{-\infty}^{\infty} dt \frac{\exp\left(-t^2\right)}{z - t} \tag{10}$$

Event-Based Cross Section Realizations

- An on-the-fly URR cross section calculation capability is implemented in OpenMC

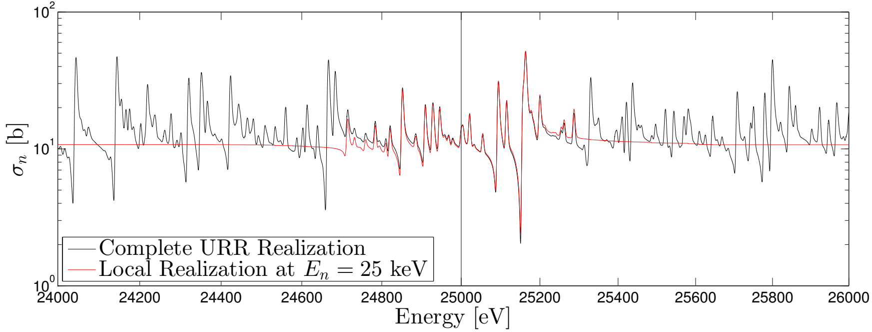

Figure : ^{238}U elastic scattering cross section realization at 25 keV

SLBW: Verification

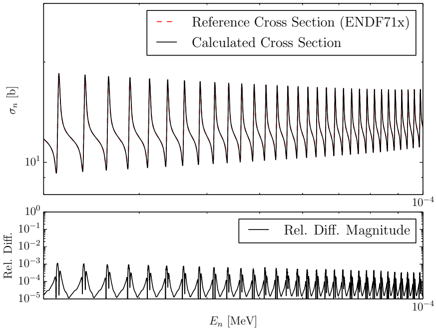

Figure : ^{239}U 293.6 K elastic scattering cross section

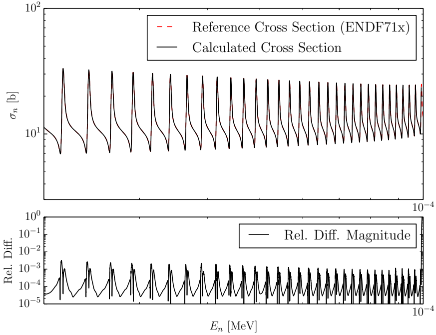

Figure : ^{243}Pu 293.6 K elastic scattering cross section

ZEBRA Critical Assembly

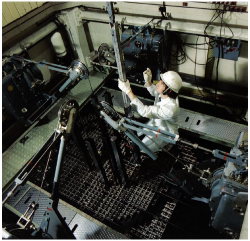

- Zero-Energy Breeder Reactor Assembly
- UK Atomic Energy Authority
- Fast reactor assemblies
- Significant URR effects (∼1000 pcm)

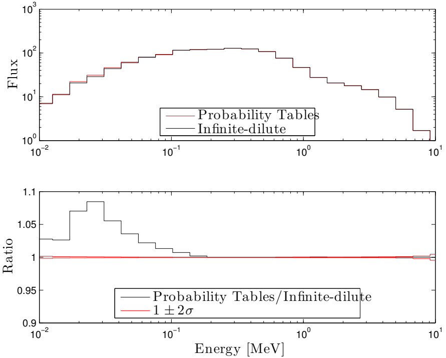

Figure : Infinite-dilute and resonance cross section flux spectra

On-the-Fly vs. Probability Tables: k_∞

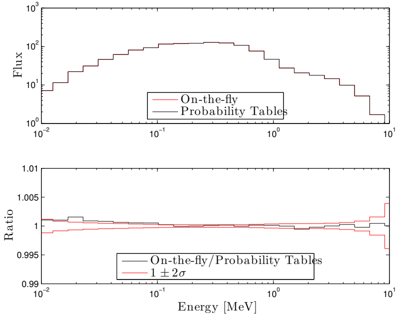

Figure : Comparison of on-the-fly and probability table flux spectra

URR Method	k_∞	1σ
Infinite-dilute	1.00914	0.00005
ENDF71x Tables	1.01897	0.00004
On-the-fly	1.01892	0.00004

Table : ZEBRA k_∞ comparison for various URR treatments

- OTF eliminates the need for pre-processing and storage of temperature-dependent probability table data
- $\sim 1000X$ memory reduction
- $\sim 0.1 - 10X$ particle simulation rate slowdown

Temperature-Dependent Probability Tables

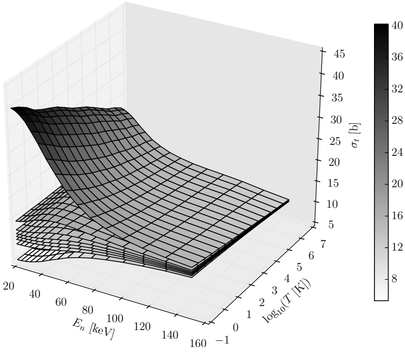

Figure : Equiprobable cross section magnitude surfaces

- Generate equiprobable cross section magnitude surfaces on an $E_n - T$ mesh
- Randomly sample magnitude and interpolate on mesh
- Compromise between typical probability table and fully OTF procedures

Temperature-Dependent Probability Tables

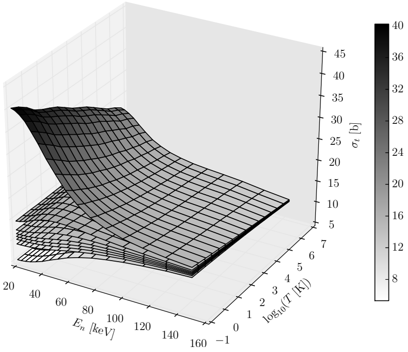

Figure : Equiprobable cross section magnitude surfaces

- Generate equiprobable cross section magnitude surfaces on an $E_n - T$ mesh
- Randomly sample magnitude and interpolate on mesh
- Compromise between typical probability table and fully OTF procedures

ΔT [K]	k_{eff}	1σ
0	1.00466	0.00010
100	1.00463	0.00010
200	1.00468	0.00010
400	1.00533	0.00010

Table : Big Ten k_{eff} for various URR treatments

Section 3

Alternate Cross Section Representations

Multi-Level Resonance Formalisms

- ENDF-6 format specifies use of SLBW for the URR
- Level-level interference is neglected
- Negative elastic scattering cross sections are possible in the resonance dips
- Multi-level Breit-Wigner (MLBW) capability implemented in OpenMC (probability tables, on-the-fly, pointwise)

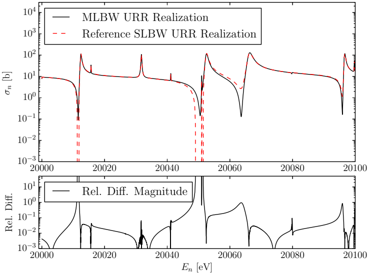

Figure : Comparison of SLBW and MLBW elastic scattering cross sections

Multi-Level Resonance Formalisms

- ENDF-6 format specifies use of SLBW for the URR
- Level-level interference is neglected
- Negative elastic scattering cross sections are possible in the resonance dips
- Multi-level Breit-Wigner (MLBW) capability implemented in OpenMC (probability tables, on-the-fly, pointwise)

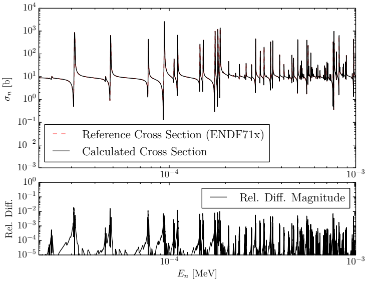

Figure : ^{234}U 293.6 K elastic scattering cross section

Multi-Level Resonance Formalisms

- ENDF-6 format specifies use of SLBW for the URR
- Level-level interference is neglected
- Negative elastic scattering cross sections are possible in the resonance dips
- Multi-level Breit-Wigner (MLBW) capability implemented in OpenMC (probability tables, on-the-fly, pointwise)

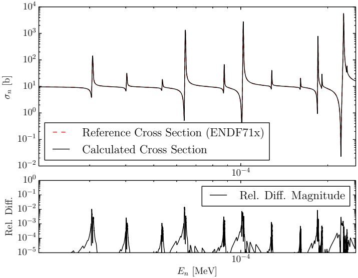

Figure : ^{244}Pu 293.6 K elastic scattering cross section

Multi-Level Resonance Formalisms

- ENDF-6 format specifies use of SLBW for the URR
- Level-level interference is neglected
- Negative elastic scattering cross sections are possible in the resonance dips
- Multi-level Breit-Wigner (MLBW) capability implemented in OpenMC (probability tables, on-the-fly, pointwise)

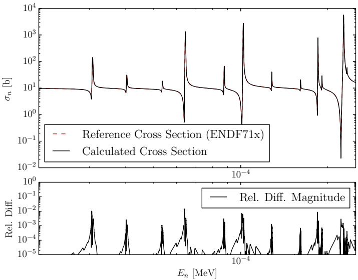

Figure : ^{244}Pu 293.6 K elastic scattering cross section

Formalism	k_{eff}	1σ
SLBW	1.00461	0.00010
MLBW	1.00453	0.00009

Table : Big Ten k_{eff} for various URR treatments, 293.6 K

Independent, Pointwise Realizations

- Calculation of **True** expected values requires independent simulations, each using a single, independent resonance structure
- Pointwise URR cross section reconstruction capability implemented in OpenMC

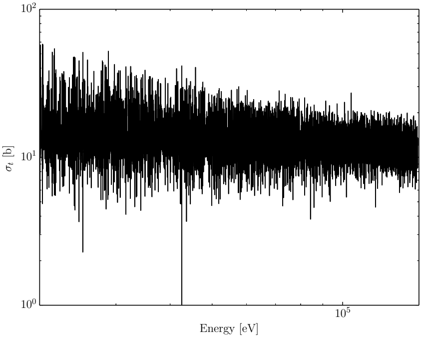

Figure : ^{238}U total cross section at 293.6 K

Independent, Pointwise Realizations

- Calculation of **True** expected values requires independent simulations, each using a single, independent resonance structure
- Pointwise URR cross section reconstruction capability implemented in OpenMC

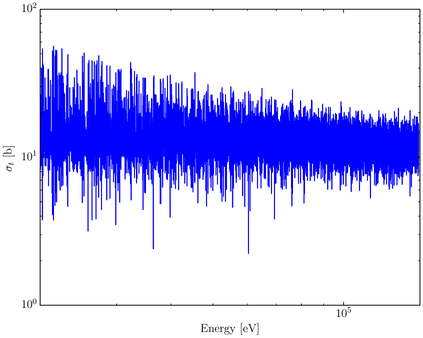

Figure : ^{238}U total cross section at 293.6 K

Independent, Pointwise Realizations

- Calculation of **True** expected values requires independent simulations, each using a single, independent resonance structure
- Pointwise URR cross section reconstruction capability implemented in OpenMC

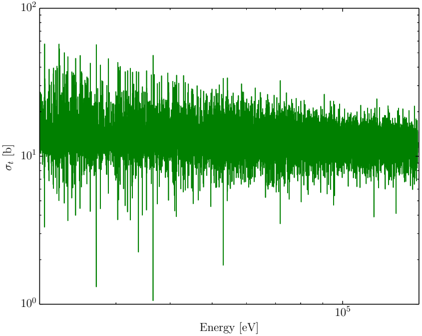

Figure : ^{238}U total cross section at 293.6 K

Independent, Pointwise Realizations

- Calculation of **True** expected values requires independent simulations, each using a single, independent resonance structure
- Pointwise URR cross section reconstruction capability implemented in OpenMC

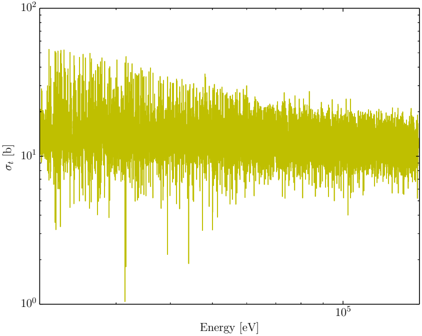

Figure : ^{238}U total cross section at 293.6 K

Independent, Pointwise Realizations

- Calculation of **True** expected values requires independent simulations, each using a single, independent resonance structure
- Pointwise URR cross section reconstruction capability implemented in OpenMC

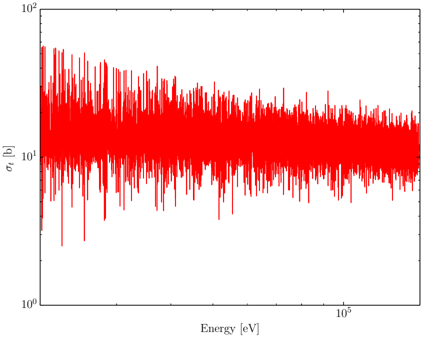

Figure : ^{238}U total cross section at 293.6 K

Independent, Pointwise Realizations

- Calculation of **True** expected values requires independent simulations, each using a single, independent resonance structure
- Pointwise URR cross section reconstruction capability implemented in OpenMC

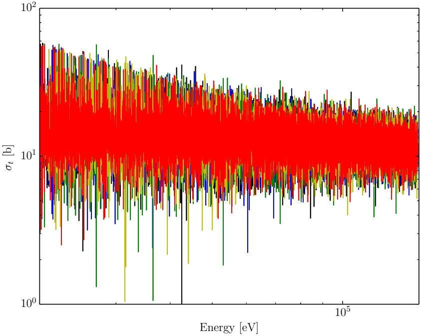

Figure : ^{238}U total cross section at 293.6 K

Independent, Pointwise Realizations

- Calculation of **True** expected values requires independent simulations, each using a single, independent resonance structure
- Pointwise URR cross section reconstruction capability implemented in OpenMC
- Probability tables reproduce expected values remarkably well (not required by theory)
- Spread of individual variates can be significant, 100's pcm on k_{eff}

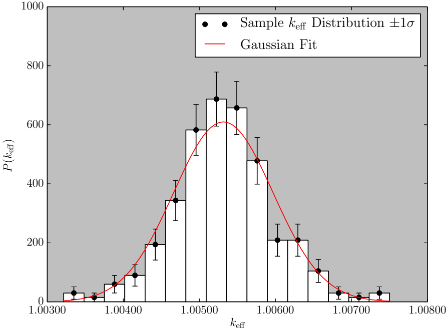

Figure : Distribution of Big Ten k_{eff} from independent URR realizations

Extended URR Evaluations

- Fast spectrum system fluxes often peak above the URR

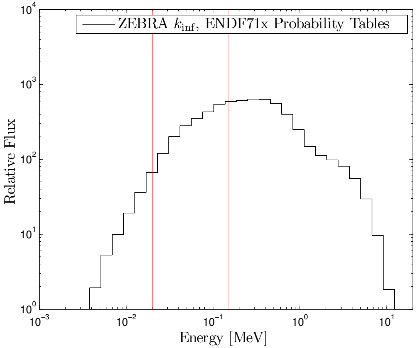

Figure : ZEBRA flux spectrum w/ ^{238}U URR highlighted

Extended URR Evaluations

- Fast spectrum system fluxes often peak above the URR
- There can still be resonance structure up there

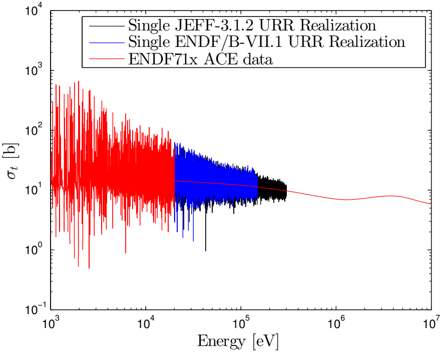

Figure : RRR and URR ^{238}U total cross sections, 293.6 K

Extended URR Evaluations

- Fast spectrum system fluxes often peak above the URR
- There can still be resonance structure up there
- Neglect of resonance structure can strongly affect integral tallies
- Are there any evaluators in the room?!

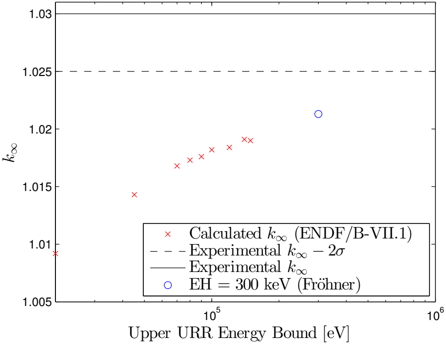

Figure : ZEBRA k_∞ variation with EH

Competitive Reaction Resonance Structure

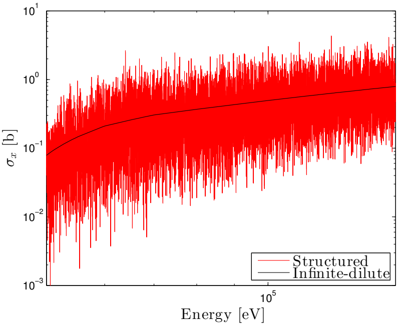

Figure : ^{238}U first-level inelastic scattering resonance structure

- Competitive reactions (e.g. level inelastic scattering) have resonance structure
- ENDF-6 format allows a single competitive width
- Resonance structure cannot be accounted for properly if two competitive channels are open
- In practice, **ALL** competitive resonance structure is often neglected

Competitive Reaction Resonance Structure

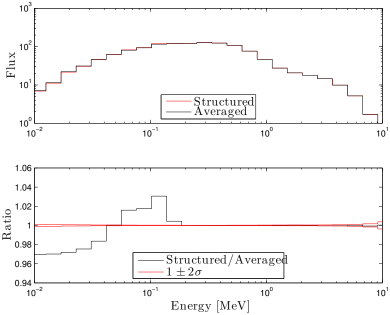

Figure : Flux spectra comparison

System	Competitive Cross Section	k_{eff}	1σ
Big Ten	Averaged	1.00459	0.00004
Big Ten	Resonant	1.00524	0.00005
ZEBRA	Averaged	1.01892	0.00004
ZEBRA	Resonant	1.02054	0.00004

Table : k_{eff} comparison for averaged and structured competitive cross sections, 293.6 K

- Competitive reactions (e.g. level inelastic scattering) have resonance structure
- ENDF-6 format allows a single competitive width
- Resonance structure cannot be accounted for properly if two competitive channels are open
- In practice, **ALL** competitive resonance structure is often neglected

Section 4

Doppler Broadening Secondary Distributions

Motivation

Methods for Processing ENDF/B-VII with NJOY (my emphasis)

"The code uses the input value **thnmax**, or the **upper limit of the resolved-resonance energy range**, or **the lowest threshold (typically$>$100 keV)** as a breakpoint. **No Doppler broadening or energy-grid reconstruction is performed above that energy**. No broadening of thresholds is normally done, **because we dont have methods to calculate the scattering distributions** from broadened thresholds. There is an option to override this for applications like astrophysics that might desire to compute reaction rates for broadened thresholds."

Motivation

Methods for Processing ENDF/B-VII with NJOY (my emphasis)

"The code uses the input value **thnmax**, or the **upper limit of the resolved-resonance energy range**, or **the lowest threshold (typically$>$100 keV)** as a breakpoint. **No Doppler broadening or energy-grid reconstruction is performed above that energy**. No broadening of thresholds is normally done, **because we dont have methods to calculate the scattering distributions** from broadened thresholds. There is an option to override this for applications like astrophysics that might desire to compute reaction rates for broadened thresholds."

- Doppler broadening of fast energy region cross sections – and reaction kernels, in general – is being restricted by an inability to broaden secondary distributions consistently

Doppler Broadened Fast Region Cross Sections

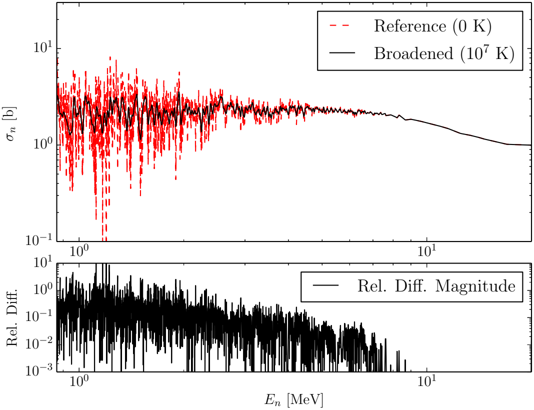

Figure : Comparison of broadened ^{56}Fe elastic scattering cross section with 0 K reference

Reaction Kernel Broadening

- Typical formulation of Doppler broadening rigorously preserves integrated reaction rate for reaction x:

$$v\sigma_x(T,v) = \int_{\forall \vec{v}_t} \mathrm{d}\vec{v}_t V(T,\vec{v}_t) v_{\mathrm{rel}} \sigma_x(0, v_{\mathrm{rel}}) \tag{11}$$

- Note: it is common to factorize $V(T,\vec{v}_t)$ into independent distributions for μ_{in} and $|\vec{v}_t|$, as in the Maxwell-Boltzmann ideal gas model
- The effective, temperature-dependent cross section, $\sigma_x(T,v)$, is used to determine where in phase-space a reaction of type x occurs

Reaction Kernel Broadening

- Typical formulation of Doppler broadening rigorously preserves integrated reaction rate for reaction x:

$$v\sigma_x(T,v) = \int_{\forall \vec{v}_t} \mathrm{d}\vec{v}_t \, V(T,\vec{v}_t) v_{\mathrm{rel}} \sigma_x(0, v_{\mathrm{rel}}) \tag{11}$$

- Note: it is common to factorize $V(T,\vec{v}_t)$ into independent distributions for μ_{in} and $|\vec{v}_t|$, as in the Maxwell-Boltzmann ideal gas model
- The effective, temperature-dependent cross section, $\sigma_x(T,v)$, is used to determine where in phase-space a reaction of type x occurs
- But, we also need to know the differential nature of the individual reaction events that occur (e.g. $\vec{v}_t$, μ_{out})

Secondary Angular Distributions

- Nuclear data evaluations provide 0 K secondary angular distributions (sometimes implicitly via Legendre coefficients)
- It is common practice to independently sample these 0 K distributions
- Implicit assumption that distributions do not have significant energy dependence

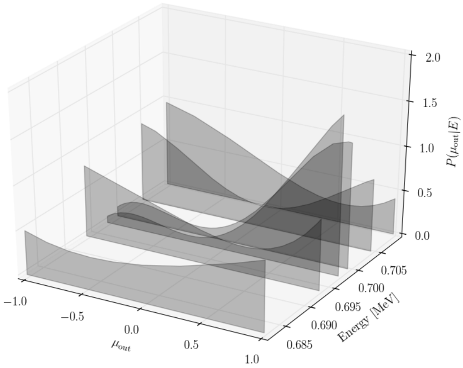

Figure : ^{56}Fe elastic scattering angular distribution

Broadening Angular Distributions

- Without loss of generality, the μ_{out}-integrated cross section, $\sigma_x(0, v_{\mathrm{rel}})$, can be expanded into its angular components

$$v\sigma_x(T, v) = \int_{\forall \vec{v}_t} \mathrm{d}\vec{v}_t \int_{-1}^{1} \mathrm{d}\mu_{\mathrm{out}} V(T, \vec{v}_t) v_{\mathrm{rel}} P(\mu_{\mathrm{out}}|v_{\mathrm{rel}}) \sigma_x(0, v_{\mathrm{rel}}) \tag{12}$$

- Integrand and a normalization constant constitute, by definition, a probability density function for the **consistent, Doppler broadened double-differential reaction kernel**

$$P(\vec{v}_t, \mu_{\mathrm{out}}|v) = \frac{1}{v\sigma_x(T, v)} V(T, \vec{v}_t) v_{\mathrm{rel}} P(\mu_{\mathrm{out}}|v_{\mathrm{rel}}) \sigma_x(0, v_{\mathrm{rel}}) \tag{13}$$

0 K and Broadened Angular Distributions

- Integrate over $\vec{v}_t$ to obtain the broadened scattering cosine distribution and compare with the 0 K data

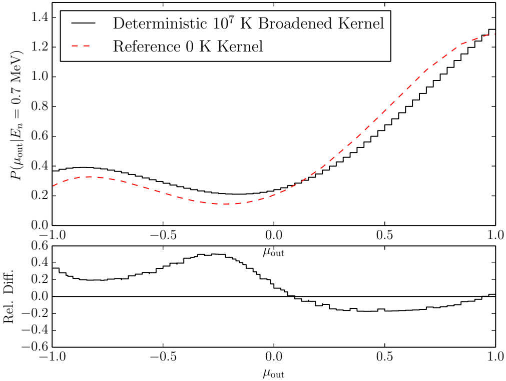

Figure : Comparison of broadened kernel with 0 K reference

0 K and Broadened Angular Distributions

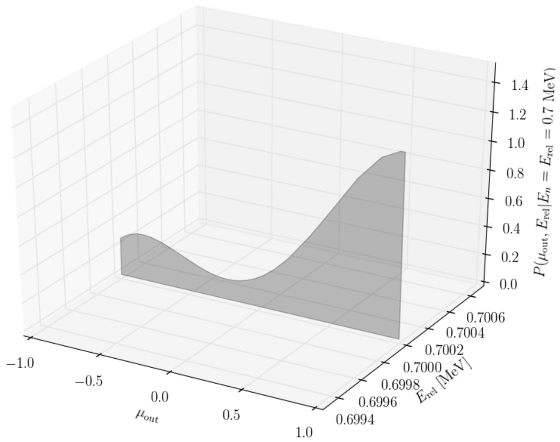

Figure : Comparison of broadened kernel with 0 K reference

0 K and Broadened Angular Distributions

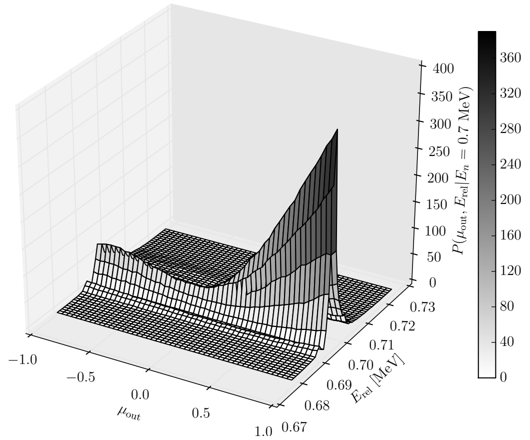

Figure : Comparison of broadened kernel with 0 K reference

Reaction Kernel Broadening Methods

- $P(\vec{v}_t, \mu_{\mathrm{out}}|v)$ can be deterministically Doppler broadened, as was previously shown
- Broadened kernels can then be straightforwardly sampled in Monte Carlo simulations
- Such a treatment is perfectly legitimate and an improvement over the state of the practice
- However, the kernels are only exact at the precise temperature to which they are broadened
- What about multiphysics? Possibly dramatic increase in secondary distribution memory requirements

Reaction Kernel Broadening Methods

- $P(\vec{v}_t, \mu_{\mathrm{out}}|v)$ can be deterministically Doppler broadened, as was previously shown
- Broadened kernels can then be straightforwardly sampled in Monte Carlo simulations
- Such a treatment is perfectly legitimate and an improvement over the state of the practice
- However, the kernels are only exact at the precise temperature to which they are broadened
- What about multiphysics? Possibly dramatic increase in secondary distribution memory requirements
- **An entirely equivalent stochastic sampling method is derived and implemented in OpenMC**
- **No memory requirement penalty incurred – 0 K data only**

Verification

- Excellent agreement between stochastic and deterministic kernels

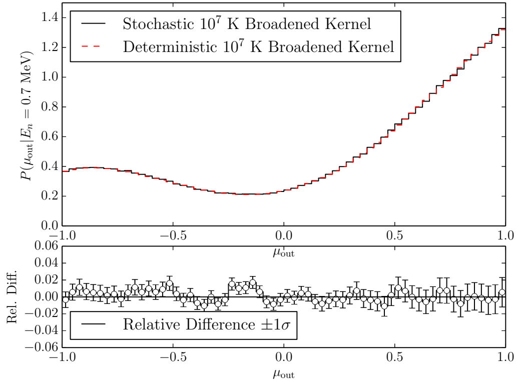

Figure : Comparison of stochastic and deterministic broadened kernels

Integral Simulations

- The stochastic kernel broadening method has been implemented for elastic scattering in the continuous-energy neutron transport code OpenMC
- Preliminary studies of integral effects are underway
  - ^{239}Pu sphere reflected by ^{56}Fe
  - Negligible bias at room temperature at the few-pcm level
  - $+609 \pm 10$ pcm bias at 10^7 K
- Suggestions for systems in which this effect is important?
- Design criteria:
  - High-temperatures to get secondary distributions that change over the range of attainable relative energies
  - Fast spectra typically needed to reach structured (i.e. non-isotropic) scattering distributions
  - ^{56}Fe, ^{9}Be, C, possibly others

Conclusions

- A flexible probability table interpolation scheme has been implemented and tested with results comparing favorably to the continuous phase-space on-the-fly approach

Conclusions

- A flexible probability table interpolation scheme has been implemented and tested with results comparing favorably to the continuous phase-space on-the-fly approach

- Several alternate resonance data representations have been implemented and tested with results showing varying degrees of significance

Conclusions

- A flexible probability table interpolation scheme has been implemented and tested with results comparing favorably to the continuous phase-space on-the-fly approach
- Several alternate resonance data representations have been implemented and tested with results showing varying degrees of significance
- A fully consistent, memory-efficient stochastic method for Doppler broadening of the double-differential elastic scattering kernel has been derived, implemented, and verified

Future Work

- Continued analyses with the presented methods
- Extend Doppler broadening of reaction kernels
  - Secondary angular distributions for other reactions
  - Secondary energy distributions
  - Correlated angle-energy distributions
- **Validation** of double-differential broadening?
- Extended URR evaluation?
- Graduate?

Acknowledgments

- XCP-3
- Forrest Brown, Ben Forget, Kord Smith, Brian Kiedrowski
- This material is based upon work supported by a Department of Energy Nuclear Energy University Programs Graduate Fellowship
- This research is partially supported by the Consortium for Advanced Simulation of Light Water Reactors (CASL), an Energy Innovation Hub for Modeling and Simulation of Nuclear Reactors under U.S. Department of Energy Contract No. DE-AC05-00OR22725